Quasi-stationary distributions for stochastic processes with an absorbing state

Ronald Dickman† and Ronaldo Vidigal

Departamento de Física, ICEx, Universidade Federal de Minas Gerais, 30123-970 Belo Horizonte - MG, Brasil

(February 1, 2008)

Abstract

We study the long-time behavior of stochastic models with an absorbing state, conditioned on survival. For a large class of processes, in which saturation prevents unlimited growth, statistical properties of the surviving sample attain time-independent limiting values. We may then define a *quasi-stationary* probability distribution as one in which the ratios $p_n(t)/p_m(t)$ (for any pair of nonabsorbing states n and m), are time-independent. This is not a true stationary distribution, since the overall normalization decays as probability flows irreversibly to the absorbing state. We construct quasi-stationary solutions for the contact process on a complete graph, the Malthus-Verhulst process, Schlögl's second model, and the voter model on a complete graph. We also construct the master equation and quasi-stationary state in a two-site approximation for the contact process, and for a pair of competing Malthus-Verhulst processes.

PACS: 05.10.Cg, 02.50.Ga, 05.40.-a, 05.70.Ln

Short title: Quasi-stationary distributions

†electronic address: dickman@fisica.ufmg.br

I. INTRODUCTION

Stochastic processes with an absorbing state arise frequently in statistical physics [1,2], epidemiology [3], and related fields. On one hand we have autocatalytic processes (in lasers, chemical reactions, or surface catalysis, for example), and population models (in genetic or epidemiological modeling), in which a population of $n \geq 0$ individuals goes permanently extinct when the absorbing state, $n = 0$, is reached. On the other hand, phase transitions to an absorbing state in spatially extended systems , exemplified by the contact process [4], are currently of great interest in connection with self-organized criticality [5], the transition to turbulence [6], and, more generally, issues of universality in nonequilibrium critical phenomena [7,8]. Such models are fequently studied using deterministic mean-field equations, Monte Carlo simulation, and renormalization group analyses.

While fluctuations play an essential role in the vicinity of the absorbing state, exact solution of the master equation is not, in general, feasible. A useful tool in this situation is van Kampen's Ω-expansion in inverse powers of the system size, about the deterministic, macroscopic solution. It is clearly desirable to develop additional methods for analyzing processes with absorbing states. In this work we study models whose macroscopic equation admits a nonabsorbing (or *active*) stationary state, but which, for a finite system size, must always end up in the absorbing state. We show that the *quasi-stationary* distribution for such a system is readily constructed, and that it provides a wealth of information about its behavior. In fact, simulations of "stationary" properties of lattice models with an absorbing state actually study the quasi-stationary regime, since the only true stationary state (for a finite system) is the absorbing one.

For models without spatial structure, such as uniformly distributed populations, well stirred chemical reactors, or networks in which each node communicates equally with all others, our results provide a complete description of long-time properties, conditioned on survival. In models with spatial structure, typified by nearest-neighbor interactions on a lattice, as in the contact process, the description in terms of one or a few variables corresponds to a mean-field theory that cannot adequately capture critical fluctuations. Our approach does, nonetheless, allow one to put some of the fluctations "back into" mean-field theory, and so we are able to study finite size effects and moment ratios that are beyond the grasp of simpler approaches. For one-step models involving a single variable, the computational demands of our approach are trivial; more complicated processes can be analyzed using straightforward numerical procedures.

The idea of the quasi-stationary state or distribution is quite simple. Consider a Markov chain $n_t \geq 0$ in continuous time, with $n = 0$ absorbing, and such that the macroscopic or rate-equation description (i.e., neglecting fluctuations) admits an active stationary state ($n_{st} > 0$). Then in many cases one expects the probability distribution $p_n(t)$ to bifurcate, after some initial transient, into two components,

one with all weight on the absorbing state, the other, $q_n(t)$, concentrated near the macroscopic value n_{st}, such that $p_n \approx 0$ for $n \simeq 0$. The survival probability (for the process not to have fallen into the absorbing state), is $P(t) = \sum_{n\geq 1} q_n(t)$. We study the case in which q_n has attained a time-independent form, in which its only time dependence is through the overall factor $P_s(t)$. Since the probability distribution is supposed to bifurcate, we may write

$$p_n(t) = Q(t)\delta_{n,0} + q_n(t) \tag{1}$$

where $Q(t) = 1 - P(t)$, and by definition, $q_0(t) = 0$. The quasi-stationary distribution (QS) is then defined via the condition:

$$p_n(t) = P(t)\overline{p}_n, \quad (n \geq 1), \tag{2}$$

where the $\overline{p}_n$ are time independent. (Again, $\overline{p}_0 \equiv 0$.) Since $P(t)$ is the survival probability we have the normalization:

$$\sum_{n\geq 1} \overline{p}_n = 1. \tag{3}$$

Clearly, not every process with an absorbing state admits a QS distribution. The exponential decay process (with transition rates $W_{n,m} = m\delta_{n,m-1}$) and the birth-and-death process ($W_{n,m} = m\delta_{n,m-1} + m\lambda\delta_{n,m+1}$), for example, do not. While we will not try to determine rigorously the conditions under which a QS distribution exists, it seems reasonable to suppose that the macroscopic equation for the process in question admits an active stationary solution. All of the examples considered satisfy this condition. The voter model represents a special case, in which the macroscopic equation provides no information on the fate of the process, and the QS distribution bears no resemblance to the stationary (absorbing) distribution.

The balance of this paper is organized as follows. In Sec. 2 we illustrate the evaluation of the QS distribution, and the analysis of associated statistical properties, for the simple case of the contact process on a complete graph. Sec. 3 is concerned with the closely related Malthus-Verhulst process (MVP). Both the contract process and the MVP exhibit a continuous phase transition in the infinite-size limit. In Secs. 4 and 5 we study a models with a discontinuous phase transition: the second Schlögl process, and the voter model. In Sec. 6 we return to the contact process, this time in a two-site approximation, and in Sec. 7 study a pair of competing MVPs. Sec. 8 contains a summary and discussion of our results.

II. CONTACT PROCESS ON A COMPLETE GRAPH

In the contact process (CP) [4,7], each site of a lattice is either occupied ($\sigma_i(t) = 1$), or vacant ($\sigma_i(t) = 0$). Transitions from $\sigma_i = 1$ to $\sigma_i = 0$ occur at a rate of

unity, independent of the neighboring sites. The reverse can only occur if at least one neighbor is occupied: the transition from $\sigma_i = 0$ to $\sigma_i = 1$ occurs at a rate of λm, where m is the fraction of nearest neighbors of site i that are occupied; thus the state $\sigma_i = 0$ for all i is absorbing. The stationary order parameter ρ (the fraction of occupied sites), is zero for $\lambda < \lambda_c$. It is easy to show that in mean-field approximation (i.e., treating occupancy of sites as statistically independent events, and supposing that the density $\rho(t)$ is spatially uniform), the density follows the rate equation:

$$\frac{d\rho}{dt} = (\lambda - 1)\rho - \lambda\rho^2 \; . \tag{4}$$

This equation predicts a continuous phase transition (from $\rho \equiv 0$ to $\rho = 1 - \lambda^{-1}$ in the stationary state) at $\lambda_c = 1$. While this is qualitatively correct, λ_c is in general larger than 1; $\lambda_c = 3.29785(2)$ in one dimension, for example.

A mean-field description such as Eq. (4) does not, of course, yield correct critical exponents for dimension $d < d_c = 4$, but that is not of concern here. Instead, we would like to study the simplest stochastic process for which Eq. (4) represents the macroscopic limit, (i.e., the limit of an infinite system, in which $\rho(t)$ is a deterministic variable). By studying such a process we can recover the fluctuations ignored in the macroscopic equation. Since the process has an absorbing state, its limiting ($t \to \infty$) distribution is trivial ($p_n(t) \to \delta_{n,0}$), but we can study the long-time properties, conditioned on survival, using the QS distribution.

The stochastic birth-and-death process whose macroscopic limit is given by Eq. (4) is the *contact process on a complete graph*, in which the rate for a vacant site to turn occupied is λ times the fraction of *all* sites that are occupied, rather than the fraction of nearest neighbors. Since each site interacts equally with all others, all pairs of sites are neighbors, defining a complete graph. Given its connections with epidemic modeling and percolation, this model has also been called "percolitis" [9].

The state of the process is specified by a single variable n: the number of occupied or infected sites. This is a one-step process with nonzero transition rates

$$W_{n-1,n} = n \tag{5}$$

$$W_{n+1,n} = \lambda \frac{n}{\Omega}(\Omega - n) \tag{6}$$

on a graph of Ω sites. These expressions yield the master equation

$$\frac{dp_n}{dt} = (n{+}1)p_{n+1} + (n{-}1)\overline{\lambda}(\Omega - n + 1)p_{n-1} - \left[1 + \overline{\lambda}(\Omega - n)\right] np_n \; , \tag{7}$$

where $\overline{\lambda} \equiv \lambda/\Omega$. Since $P(t) = \sum_{n\geq 1} p_n(t)$, we have $dP/dt = -p_1(t)$ in the contact process, and under the QS hypothesis,

$$\frac{1}{P}\frac{dP}{dt} = -\overline{p}_1. \tag{8}$$

If we insert Eq. (2) in the master equation, then, dividing through by $P(t)$ we obtain

$$\overline{\lambda}(n-1)[\Omega-n+1]\overline{p}_{n-1} + (n+1)\overline{p}_{n+1} - [\overline{\lambda}(\Omega-n)+1]n\overline{p}_n + \overline{p}_1\overline{p}_n = 0, \tag{9}$$

for $n \geq 1$. For a given n, Eq. (9) furnishes a relation for $\overline{p}_{n+1}$ in terms of $\overline{p}_n$ and $\overline{p}_{n-1}$. Letting $u_n = n[\overline{\lambda}(\Omega-n)+1]$, we have

$$\overline{p}_2 = \frac{1}{2}\overline{p}_1(u_1 - \overline{p}_1) \tag{10}$$

and

$$\overline{p}_n = \frac{1}{n}\left[(u_{n-1} - \overline{p}_1)\overline{p}_{n-1} + (n-2)(\Omega-2)\overline{\lambda}\overline{p}_{n-2}\right] \tag{11}$$

for $n = 2, ..., \Omega$. Thus the QS distribution is completely determined once $\overline{p}_1$ is known; the latter is determined via the normalization condition, Eq. (3).

In practice the following iterative scheme converges very quickly. Starting with a guess for $\overline{p}_1$ (unity, for instance), one uses the recurrence relations to find the corresponding $\overline{p}_n$, and then evaluates $S = \sum_{n=1}^{\Omega} p_n$. The procedure is then repeated using $\overline{p}_1' = \overline{p}_1/S$; after a modest number of steps, S converges to unity, at which point the $\overline{p}_n$ represent the QS distribution.

We have confirmed that the master equation for the contact process on a complete graph does in fact attain the QS distribution at long times. We integrate the master equation using a fourth-order Runge-Kutta scheme [10], and stop the integration when the mean population conditioned on survival, $\langle n \rangle_s = \sum_n np_n(t)/P(t)$, changes by less than 10^{-10} per time step. The resulting distribution, $p_n^* = p_n(t)/P(t)$ is compared with the QS distribution furnished via the recurrence relations in figure 1; they are identical.

Having constructed the QS distribution and verified that it indeed represents the long-time distribution (conditioned on survival), as given by the master equation, we now examine some properties of the QS state. Figure 2 shows the quasi-stationary population density $\rho = n/\Omega$ versus λ for various system sizes. This plot looks strikingly similar to finite-size plots of the order parameter at a continuous phase transition. In particular, it is evident that the λ-dependence is smooth for any finite system, but that on increasing Ω, the function $\rho(\lambda, \Omega)$ approaches a singular limit.

On finite-dimensional lattices the value of the order parameter at the critical point is expected to scale as $\rho(\lambda_c, \Omega) \sim \Omega^{-\beta/\nu_\perp}$, where β and $\nu_\perp$ are the critical

exponents governing the order parameter and the divergence of the correlation length [7]. Here we find $\rho(\lambda_c, \Omega) \approx 0.685\Omega^{-1/2}$ (from results for $\Omega = 500 - 10^5$). We note that the mean-field exponent values $\beta = 1$ and $\nu_\perp = 1/2$ for the contact process would lead one to expect $\rho(\lambda_c, \Omega) \sim \Omega^{-2}$. The reason for the difference would seem to be that on a complete graph (where each site is, in effect, a unit distance from all others), the correlation length is undefined, and so finite-size scaling ideas do not apply. Instead, we can understand the exponent -1/2 by noting that the microscopic equation (4), gives $\rho = 0$ at the critical point, so that n is purely a fluctuation. The central limit theorem then requires $n \sim \Omega^{1/2}$. Away from the critical point, $\lambda = 1$, the finite-size correction to the mean-field solution, $\rho = 1 - \lambda^{-1}$, is $\mathcal{O}(\Omega^{-1})$.

Another property of interest at a continuous phase transition is the moment ratio $m = \langle n^2 \rangle / \langle n \rangle^2$. This quantity is analogous to Binder's reduced fourth cumulant [11], at an equilibrium critical point: the curves $m(\lambda, \Omega)$ for various Ω cross near λ_c (the crossings approach λ_c), so that m assumes a universal value m_c at the critical point. For the basic contact process (and other models in the universality class of directed percolation), $m_c = 1.174$ and 1.326 in one and two dimensions, respectively [12]. In figure 3 we plot m for the quasi-stationary contact process on a complete graph. Qualitatively, the behavior is similar to that observed on finite-dimensional lattices, with $m(\lambda)$ becoming ever steeper with increasing system size; $|dm/d\lambda|_{\lambda_c} \sim \Omega^{1/2}$ for large Ω. The crossings approach λ_c, as expected. We find that $m(1, \Omega) \simeq 1.660 + \mathcal{O}(\Omega^{-1/2})$ for large Ω.

As noted above, the survival probability decays as $dP(t)/dt = -p_1(t)$. We may therefore interpret $\overline{p}_1$ as the quasi-stationary decay rate. The QS lifetime, $\tau = 1/\overline{p}_1$, grows as exp[const. $\Omega(\lambda - \lambda_c)$] for $\lambda > \lambda_c$, as can be seen from figure 4, where we plot $\Omega^{-1} \ln \tau$ versus λ for several system sizes. At the critical point, $\tau \sim \Omega^{1/2}$.

It may appear surprising that we are able to discuss quasi-stationary properties for $\lambda < \lambda_c$, where an active stationary state does not exist, even in the thermodynamic limit. The existence of nontrivial QS properties for $\lambda < \lambda_c$ is in fact a finite-size effect, analogous to a nonzero magnetization in the Ising model above the critical temperature, on a finite lattice. For $\lambda > \lambda_c$ the QS state converges, as $\Omega \to \infty$, to the true stationary state, while for $\lambda < \lambda_c$ it converges to the absorbing state. But since the properties of any *finite* system are nonsingular, we must expect a smooth decay of, for example, the density, as $\lambda \to 0$.

A. Pseudo-stationary distribution

The contact process on a finite graph (be it a regular lattice, a complete graph, or small-world network) has only the absorbing state as its true stationary state. It is nonetheless instructive to examine the result of *forcing* a time-independent solution on the master equation. This is easily done by introducing the generating function $F(z,t) \equiv \sum_n p_n(t) z^n$. The master equation, Eq.(7), is equivalent to the

partial differential equation,

$$\frac{\partial F}{\partial t} = (1-z)\left[(1-\overline{\lambda}z)\frac{\partial F}{\partial z} + \overline{\lambda}z\frac{\partial}{\partial z}\left(z\frac{\partial F}{\partial z}\right)\right] . \tag{12}$$

Setting $\partial F/\partial t = 0$ and letting $G(z) = \partial F/\partial z$, a first integration yields

$$G(z) = Cz^{\Omega-1}e^{1/\overline{\lambda}z} , \tag{13}$$

where C is a constant. Integrating once more gives

$$F_{ps}(z) = C\sum_{n=0}^{\infty}\frac{z^{\Omega-n}}{\overline{\lambda}^n n!(\Omega-n)} . \tag{14}$$

While the corresponding distribution,

$$p_{ps,m} = \frac{C\overline{\lambda}^m}{(\Omega-m)!m} \tag{15}$$

yields $dp_m/dt = 0$ when inserted in the master equation, it is not a valid solution since it cannot be normalized, and does not satisfy the correct boundary condition at $m = 0$. For this reason we call $p_{ps,m}$ a *pseudo-stationary* distribution. Similar pseudo-stationary distributions have been derived by Muñoz from the Fokker-Planck equation for continuous versions of the contact process and of a model with multiplicative noise [13].

If we treat $p_{ps,m}$ as a proper probability distribution, restricting it to $m = 1, ..., \Omega$, and normalizing it on this set, then the resulting distribution turns out to be very close to the quasi-stationary one when p_m is negligible in the vicinity of $m = 0$. Figure 5 (for $\Omega = 100$) shows that the two distributions are essentially identical for $\lambda = 2$ (as they are for larger λ values), and for $\lambda = 1.5$, except for small n. For $\lambda = 1.2$, however, the distributions are radically different; in particular, we see that the pseudo-stationary distribution does not respect the absorbing boundary at $n = 0$.

In summary, the pseudo-stationary distribution provides a simple and useful approximation to the true QS distribution for λ (and Ω) sufficiently large that $p_m \simeq 0$ for $m \simeq 1$. (In this case the survival probability decays extremely slowly, rendering the hypothesis of a stationary distribution - while strictly incorrect - at least reasonable.) As we approach the critical value, however, the region near $n = 0$ assumes dominance, and p_{ps} bears little relation to the quasi-stationary distribution.

III. MALTHUS-VERHULST PROCESS

The Malthus-Verhulst process (MVP) is a birth-and-death type process, $n(t)$, very similar to the contact process on a complete graph, but with the difference that n may assume any nonnegative integer value. The nonzero transition rates for this one-step process are:

$$W_{n-1,n} = \mu n + \frac{\nu}{\Omega} n(n-1) \ , \tag{16}$$

$$W_{n+1,n} = \lambda n \ . \tag{17}$$

In the first expression, Ω represents the system size, as discussed by van Kampen [1]. In the MVP there is no lattice structure, and no fixed limit to the population size, as there is in the contact process; rather, growth is limited by the term $\propto \nu$, which represents competition between individuals for access to finite resources. (Thus ν represents an intrinsic competition parameter, and $(\nu/\Omega)n(n-1)$ is the rate of interactions between pairs of individuals in a system of size Ω.) The saturation effect that permits a nontrivial quasi-stationary state is imposed in the death term, whereas it appears in the birth term, in the contact process.

Letting $n = \Omega\rho$, the macroscopic equation for the MVP is

$$\frac{d\rho}{dt} = (\lambda-\mu)\rho - \nu\rho^2 \tag{18}$$

which has the stationary solution $\overline{\rho} = (\lambda-\mu)/\nu$. The master equation is

$$\frac{dp_n}{dt} = [\mu + \overline{\nu} n](n+1)p_{n+1} + (n-1)\lambda p_{n-1} - [\lambda + \mu + \overline{\nu}(n-1)]np_n \ , \tag{19}$$

with $\overline{\nu} = \nu/\Omega$. Inserting the quasistationary form of the probability distribution, one readily obtains the recurrence relation

$$\overline{p}_n = \frac{(q_{n-1} - \mu\overline{p}_1)\overline{p}_{n-1} - \lambda(n-2)\overline{p}_{n-2}}{n[\mu + \overline{\nu}(n-1)]}, \tag{20}$$

where

$$q_n = [\lambda + \mu + \overline{\nu}(n-1)]n \tag{21}$$

The QS distribution can be found using the same iterative procedure as for the contact process. (We cut off the distribution at a certain M such that $\overline{p}_{\leq} 10^{-20}$ for $n > M$.)

The quasi-stationary properties of the MVP are quite similar to those of the contact process on a complete graph. Figure 6 shows the dependence of ρ on λ for system sizes $\Omega = 100$, 10^3 and 10^4. (We fix $\mu = \nu = 1$ in all numerical studies of the MVP.) The density grows linearly with λ for $\lambda > \lambda_c = \mu$, unlike in the contact process, where the macroscopic saturation term is also proportional to the birth rate, λ. As in the contact process on a complete graph, the lifetime $\tau \sim \Omega^{1/2}$ at λ_c, and the QS density decays $\sim \Omega^{-1/2}$.

The moment ratios m (figure 6, inset) show the same qualitative trend as in the CP. The asymptotic value of m at the critical point, moreover, is the same as in the CP: we find $m \simeq 1.660 - 0.814\Omega^{-1/2}$ for large Ω. This identity of m values suggests that the limiting QS probability distributions at λ_c are the same for the two processes. This is verified numerically; for $\Omega = 10^3$, for example, the distributions differ by less than about 2×10^{-4}.

In fact, the critical QS probability distribution for the MVP (and by extension for the contact process) enjoys the scaling property

$$\overline{p}_n = \frac{1}{\sqrt{\Omega}} f(n/\sqrt{\Omega}) \ . \tag{22}$$

The scaling function f may be found using a method that parallels van Kampen's analysis of the master equation [1]. First, we treat n in Eq. (20) as a continuous variable, expanding $\overline{p}_{n\pm1}$ to second order. Setting $\lambda = \mu$ at the critical point, we obtain

$$\frac{1}{2}[(2\mu + \overline{\nu})n + \overline{\nu}n^2]\frac{d^2\overline{p}}{dn^2} + [2\mu + \overline{\nu}n(1+n)]\frac{d\overline{p}}{dn} + 2\overline{\nu}n\overline{p} = -\mu\overline{p}_1\overline{p} \ . \tag{23}$$

Next we make the change of variables $y = n/\Omega^{1/2}$, and $f(y) = \Omega^{1/2}\overline{p}_n$. This yields an expansion in inverse powers of $\Omega^{1/2}$; at lowest order (Ω^{-1}) we find

$$\mu y \frac{d^2 f}{dy^2} + [2\mu + \nu y^2]\frac{df}{dy} + 2\nu y f = -\mu f(0) f(y) \ . \tag{24}$$

The initial value $f(0)$ must be chosen such that $\int_0^\infty f dy = 1$.

To integrate Eq. (24) numerically we let $g(y) = df/dy$, and note that $g(0) = -[f(0)]^2/2$, and $dg/dy|_{y=0} = -(2\nu/\mu)f(0)$. Setting $\mu = \nu = 1$, numerical integration yields the scaling function shown in figure 7, which agrees well with the distributions for the MVP and the contact process on a complete graph, in the limit of large system size. [Note that the change of variables used to derive Eq. (24) yields the very same equation when applied to the recursion relation for the contact process, Eq. (9), at its critical point, $\lambda = 1$.] The asymptotic scaling function $f(y)$ yields the moment ratio $m = 1.660063$, again in agreement with results from the recurrence relations. (Note that $m = f(0)/\langle y \rangle$, as may be verified directly from Eq. (24).)

Despite some superficial differences, the MVP and the contact process on a complete graph show the same type of phase transition (continuous, with mean-field-like critical exponents), in the limit $\Omega \to \infty$, and the same scaling properties at their respective critical points.

As in the case of the contact process, one may define a pseudo-stationary distribution by demanding that the r.h.s. of the master equation be zero. The resulting expression,

$$p_{ps,n} = C \frac{(\lambda/\overline{\nu})^n}{n(n+\mu/\overline{\nu}-1)!} \tag{25}$$

is very similar to that of the contact process on a complete graph, and again represents a good approximation to the quasi-stationary distribution if $\overline{p}_n \simeq 0$ for $n \simeq 1$.

IV. SCHLÖGL'S SECOND MODEL

The processes studied in the preceding sections exhibit a continuous phase transition; next we consider a process with a discontinuous transition. Schlögl's second model [14] describes the set of autocatalytic reactions $A \to 0$, $2A \to 3A$, and $3A \to 2A$ in a well stirred system. Since the growth process is quadratic in the density (rather than linear, as in the contact and MV processes), a low-density active state is unstable, and we expect a discontinuous transition to a state with a nonzero density as the growth rate is increased. The nonvanishing transition rates are:

$$W_{n-1,n} = \mu n + \frac{\nu}{\Omega^2} n(n-1)(n-2) \ , \tag{26}$$

$$W_{n+1,n} = \frac{\lambda}{\Omega} n(n-1) \ . \tag{27}$$

These yield the macroscopic equation:

$$\frac{d\rho}{dt} = -\mu\rho + \lambda\rho^2 - \nu\rho^3 \ , \tag{28}$$

which admits an active stationary solution,

$$\rho_s = \frac{1}{2}\left[\lambda + \sqrt{\lambda^2 - 4\mu\nu}\right] , \tag{29}$$

for $\lambda \geq 2\sqrt{\mu\nu}$ (The stationary density jumps from zero to $\sqrt{\mu\nu}$ at the transition. It is known that in a spatially extended system the transition is actually continuous for $d < 4$ [16,15], but here we treat the well stirred system, which exhibits a discontinuous phase transition.)

Since this is a one-step process, it is a simple matter to derive the recurrence relations for the quasi-stationary probabilities:

$$\overline{p}_n = \frac{(q_{n-1} - \mu\overline{p}_1)\overline{p}_{n-1} - \overline{\lambda}(n-2)(n-3)\overline{p}_{n-2}}{n[\mu + \overline{\nu}(n-1)(n-2)]} \tag{30}$$

where

$$q_n = [\mu + \overline{\lambda}(n-1) + \overline{\nu}(n-1)(n-2)]n \; , \tag{31}$$

with $\overline{\lambda} = \lambda/\Omega$ and $\overline{\nu} = \nu/\Omega^2$. These may be solved using the same method as for the contact process or the MVP.

In the following numerical example, we fix $\mu = \nu = 1$, and study the neighborhood of the transition at $\lambda = 2$. Figure 8 shows the quasi-stationary density near the transition; with increasing Ω the density approaches the discontinuous stationary solution, Eq. (29). The density goes from $\mathcal{O}(1/\Omega)$ to $\mathcal{O}(1)$, in a transition region of width $\sim \Omega^{-1/2}$. The moment ratio m, at the transition, appears to approach unity (from above) slowly, as $\Omega \to \infty$; data for $\Omega \leq 5 \times 10^4$ yield $m \simeq 1 + 2.64\Omega^{0.265}$. Similarly, the density at the transition approaches its limiting value from below: $\rho \simeq 1 - 1.5\Omega^{0.211}$. The lifetime at the transition appears to grows as $\tau \simeq \Omega^{0.35}$. Essentially the same power laws (but with different prefactors) are found at the transition for $\mu = 2$ and $\nu = 1/2$.

The probability distribution is bimodal in the neighborhood of the transition, a hallmark of a discontinuous transition. This is evident in figure 9, where the relative amplitudes of the two peaks, one at $n = 1$, the other near $n \simeq 1000$, shift rapidly near the transition. The bimodal distribution of course presages a hysteresis loop when $\Omega \to \infty$.

V. VOTER MODEL ON A COMPLETE GRAPH

A somewhat simpler model exhibiting a discontinuous phase transition is the voter model [17,18]. It differs from the systems considered previously in that it possesses *two* absorbing states. In the voter model each site on a lattice is in one of two states, A or B; each $A - B$ nearest-neighbor pair has a unit rate to change to the state AA (with probability ω) or to BB (with probability $1 - \omega$). Let $n(t)$ denote the number of sites in state A; both $n = 0$ and $n = \Omega$ are absorbing, on a lattice of Ω sites. Starting from a random initial condition with equal densities of A and B, the stationary probability distribution switches discontinuously from $\delta_{n,0}$ to $\delta_{n,\Omega}$ as ω is increased through 1/2. Of particular interest is the coarsening dynamics for $\omega = 1/2$ [18]. In this case $\langle n \rangle$ is constant, and the probabilities of the two absorbing states are determined by $n(0)$.

In this brief section we study the model on a complete graph, for the case $\omega = 1/2$. The master equation is

$$\frac{dp_n}{dt} = \frac{n-1}{2\Omega}(\Omega-n+1)p_{n-1} + \frac{n+1}{2\Omega}(\Omega-n-1)p_{n+1} - \frac{n}{2\Omega}(\Omega-n)p_n \, . \tag{32}$$

This yields the macroscopic equation $d\rho/dt = 0$, reflecting the dominance of fluctuations in this process. From the terms for $n = 0$ and $n = \Omega$ we find that in the QS state, the survival probability obeys

$$\frac{1}{P}\frac{dP}{dt} = -\frac{1}{2}(1-\Omega^{-1})(\overline{p}_1+\overline{p}_\Omega) \, , \tag{33}$$

allowing us to write the following relation for the QS distribution:

$$-\overline{p}_n(1-\Omega^{-1})(\overline{p}_1+\overline{p}_{\Omega-1}) = \frac{n-1}{\Omega}(\Omega-n+1)\overline{p}_{n-1} + \frac{n+1}{\Omega}(\Omega-n-1)\overline{p}_{n+1} - 2\frac{n}{\Omega}(\Omega-n)\overline{p}_n \, . \tag{34}$$

The solution is the uniform distribution, $\overline{p}_n = 1/(\Omega - 1)$ for $n = 1, ..., \Omega-1$ (here, $\overline{p}_0 = \overline{p}_\Omega = 0$).

In the case of the voter model, the QS distribution looks very different from the stationary distribution, even in the infinite-Ω limit. This is because the process has no active stationary state: on a complete graph it must always fluctuate into one of the absorbing states. If we exclude all trials that hit one of the boundaries, we are in effect looking at a random walker confined to an interval, whose distribution is asymptotically uniform.

VI. TWO-SITE APPROXIMATION FOR THE CONTACT PROCESS

In this section we return to the contact process, constructing a stochastic description in terms of nearest-neighbor pairs of sites, on a ring of Ω sites. The idea of the approximation is similar to that of two-site or pair mean-field dynamic mean-field theory [7], except that in the present case we treat the number of occupied sites, n, and the number of doubly-occupied nearest-neighbor pairs, z, as stochastic variables. When necessary, we invoke the usual factorization of three-site probabilities in terms of those for two sites, in order to construct the transition rates.

We begin by establishing the range of allowed values for z. Using '1' and '0' to represent occupied and vacant sites, respectively, z is the number of (11) nearest-neighbor (NN) pairs. Let w represent the number of (10) NN pairs. (For obvious reasons, the number of (01) pairs is again w.) Note that w is not an independent

variable, since each 1 is followed wither by a 0 or another 1, yielding $n = z + w$. Similarly, the number of (00) pairs v is given by $v = \Omega - 2n + z$. (Here we used $n + 2w + z = \Omega$.) Evidently v is restricted to the set $\{0, ..., \Omega\}$ while w must be in $\{0, ..., \Omega/2\}$ (We assume Ω even.) These considerations imply certain limits for z on a ring of Ω sites, as listed in table 1.

Table 1. Allowed values for z in the CP on a ring.

n	z
$0, 1$	0
$2, ..., \Omega/2$	$0, ..., n{-}1$
$\Omega/2 + 1, ..., \Omega{-}1$	$2n{-}\Omega, ..., n - 1$
Ω	Ω

Next we construct the transition rates $W_{n',z';n,z}$. From a given state (n, z) there are at most five possible transitions, viz., to the states $(n', z') = (n{-}1, z)$, $(n{-}1, z{-}1)$, $(n{-}1, z{-}2)$, $(n{+}1, z{+}1)$, and $(n{+}1, z{+}2)$. The first three represent annihilation of a particle with, resp. zero, one or two occupied nearest neighbors, while the last two represent creation of a particle at a site with one, or two occupied neighbors, resp. The rate of the transition $(n, z) \to (n{-}1, z)$ is the number of isolated particles, that is, triplets of the form (010). This number is not determined completely by n and z; we estimate it as the number of (01) pairs times the conditional probability of a vacant site given an occupied neighbor: $w \times (w/n)$. This estimate, however, is obviously wrong when $z = n - 1$ and $n \geq 2$, in which case there are *no* (010) triplets. Thus we have

$$W_{n-1,z;n,z} = \begin{cases} 0, & z = n{-}1,\ n > 1 \\ \frac{(n-z)^2}{n}, & \text{otherwise} \end{cases} \tag{35}$$

By similar arguments, we find:

$$W_{n-1,z-1;n,z} = \begin{cases} 2, & z = n{-}1,\ n > 1 \\ (n-z)\frac{2z}{n}, & \text{otherwise} \end{cases} \tag{36}$$

$$W_{n-1,z-2;n,z} = \begin{cases} 0, & z = 1 \\ n{-}2, & z = n{-}1,\ n = 3, ..., \Omega - 1 \\ \frac{z^2}{n}, & \text{otherwise} \end{cases} \tag{37}$$

$$W_{n+1,z+1;n,z} = \begin{cases} \lambda, & z = n{-}1 \\ \lambda(n-z)\frac{\Omega-2n+z}{\Omega-n}, & \text{otherwise} \end{cases} \tag{38}$$

$$W_{n+1,z+2;n,z} = \begin{cases} 0, & z = n{-}1 \\ \lambda\frac{(n-z)^2}{\Omega-n}, & \text{otherwise} \end{cases} \tag{39}$$

In the macroscopic limit, the master equation defined by these rates yields a pair of coupled equations for the particle density ρ and the pair density $\zeta = z/\Omega$ [7]. The critical value $\lambda_c{=}2$ in this approximation.

Since this is not a one-step process, we cannot obtain the QS distribution via recurrence relations, as was done in the previous examples. The most obvious approach - direct integration of the master equation - works reasonably well for modest system sizes ($\Omega < 200$ or so), but becomes very slow for large Ω. This is due in part to the large number of equations ($\sim \Omega^2$), and to the fact that the transition rates are $\mathcal{O}(\Omega)$, forcing one to use a time step $\sim \Omega^{-1}$, to avoid numerical instability. A much more efficient iterative scheme that converges directly to the QS distribution is described in Ref. [19]. The basic idea of this approach is that in the QS regime,

$$\overline{p}_n = \frac{r_n}{w_n - r_0} \ , \tag{40}$$

for any nonabsorbing state n, where $r_n = \sum_{n'} W_{n,n'} p_{n'}(t)$ is the flux of probability into state n (r_0 is the flux into the absorbing state), and $w_n = \sum_{n'} W_{n',n}$ is the total transition rate exiting n. The iterative scheme [19] starts with an arbitrary distribution p_n normalized on $n \geq 1$ (or, in the multivariate case, on the set of nonabsorbing states). Next one evaluates

$$p'_n = a p_n + (1-a) \frac{r_n}{w_n - r_0} \ , \tag{41}$$

where a is a parameter between zero and one. The new distribution p'_n is then normalized, and inserted in the r.h.s. of Eq. (41), and the process repeated until it converges. For large Ω the time to reach the QS distribution is three or more orders of magnitude smaller than that required for numerical integration. (In the present case convergence is enhanced if one uses a small value for a, e.g., 0.01. A further economy is realized by noting that, near λ_c, $\overline{p}_{nz}$ is extremely small for $n \simeq \Omega/2$, allowing one to truncate the distribution. For $\Omega = 1280$ and $\lambda = 2$, for example, $\overline{p}_{nz} \sim 10^{-17}$ for $n = 350$.)

We studied the QS properties of the contact process on a ring of $\Omega = 10$, 20, 40,..., 2560 sites, using the pair approximation. Figure 10 shows that the dependence of the particle density and the moment ratio on λ and on system size is qualitatively similar to that found in the complete graph case. The scaling laws for the density ($\propto \Omega^{-1/2}$) and the lifetime ($\propto \Omega^{1/2}$) at the critical point are the same as for the CP on a complete graph. The critical values of the moment ratio m at λ_c, extrapolated to infinite system size, yield $m_c = 1.653$, nearly the same as for the CP on a complete graph. The critical probability distribution $\overline{p_n}$ again shows a scaling collapse (figure 11), but the scaling function differs somewhat from that for the complete graph. Figure 12 shows the joint QS distribution $\overline{p}_{n,z}$ at the critical point, for $\Omega = 40$. For each n there is a most probable number, $z^*(n)$, of pairs; z^* grows linearly with n.

VII. COMPETING MALTHUS-VERHULST PROCESSES

As a final example we consider a population consisting of two types, A and B, that evolve according to the MVP analyzed in Sec. 3. (The two subpopulations may, for example, possess different alleles of a certain gene, in a species with asexual reproduction.) A and B interact via two mechanisms: (1) each individual competes with all others (regardless of type) for access to resources; (2) on reproducing, A mutates to B with probability q, and vice-versa. Thus we have the following set of transition rates:

$$W_{n_A-1,n_B;n_A,n_B} = \mu_A n_A + \frac{\nu}{\Omega} n_A(n_A+n_B-1) , \tag{42}$$

$$W_{n_A,n_B-1;n_A,n_B} = \mu_B n_B + \frac{\nu}{\Omega} n_B(n_A+n_B-1) , \tag{43}$$

$$W_{n_A+1,n_B;n_A,n_B} = \lambda_A p n_A + \lambda_B q n_B , \tag{44}$$

$$W_{n_A,n_B+1;n_A,n_B} = \lambda_B p n_B + \lambda_A q n_A , \tag{45}$$

where $p = 1-q$.

Evidently the state $n_A = n_B = 0$ is absorbing. For mutation probability $q = 0$, $n_A = 0$ is also absorbing (similarly $n_B = 0$), and in the QS state only one type is present, i.e., $\overline{p}_{n_A,n_B} = 0$ if both n_A and n_B are nonzero. This prompts us to investigate the effect of a nonzero mutation rate: Will the predominance of one species persist when mutation is possible? To address this issue we study the order parameter

$$\Delta \equiv \frac{\langle |n_A - n_B| \rangle}{\langle n_A + n_B \rangle} \tag{46}$$

in the QS state. Figure 13 shows how Δ varies with q, for various system sizes. The competing MVPs are both at the critical point, $\lambda_i = \mu_i$. (For simplicity we take all rates, λ_i, μ_i, and ν, equal to unity). The order parameter decreases with increasing mutation probability, as expected, and with increasing system size. From analysis of Δ at various q-values, as a function of Ω, it appears that $\lim_{\Omega\to\infty} \Delta(q, \Omega; \lambda_c) = 0$ for *any* nonzero q. In other words, an arbitrarily small mutation rate restores the symmetry of the process. We observe qualitatively similar behavior in $\Delta(q, \Omega)$ above the critical point ($\lambda > 1$). At the critical point, the decay of $\Delta(q, \Omega)$ with Ω is slower than exponential, but faster than a power law; it can be fit approximately by a stretched exponential $\sim \exp[-c\, \Omega^{0.2}]$, where the factor c depends on q (see figure 13 inset).

VIII. DISCUSSION

We study quasi-stationary probability distributions for Markov processes exhibing a phase transition between an active and an absorbing state. The QS distribution, which represents the long-time limit of the probability distribution, conditioned on survival, yields a complete statistical description of the process in this limit. While the QS distribution can always, in principle, be found by integrating the master equation, we present much more efficient methods for its generation: recurrence relations for one-step processes, and an iterative scheme for multi-step or multivariate processes.

Some insight into the nature of the quasi-stationary distribution is afforded by the considering the equation (in the notation of Sec. VI), for $n \geq 1$,

$$\frac{dq_n}{dt} = -w_n q_n + r_n + r_0 q_n \ , \tag{47}$$

where $r_n = \sum_{n'} W_{n,n'} q_{n'}$ is the flux of probability into state $n \geq 0$. (As usual we take state 0 as absorbing.) Without the final term on the right-hand side, this is simply the master equation. Including this term, however, the equation has as its stationary solution the QS distribution, $\overline{p}_n$. In other words, the QS distribution corresponds to the stationary state of a "process" in which all flux to the absorbing state is immediately *reinserted* into the non-absorbing subspace. The portion alloted to state n is equal to its probability, q_n.

Thus the QS distribution does not result from imposing a simple boundary condition (such as periodic, or reflection at the origin), on the original master equation. Since Eq. (47) is nonlinear, it is not a master equation. It may happen, nevertheless, that the QS distribution for a certain process (possessing an absorbing state), is also the *stationary* distribution for some other process, as in fact was found for the voter model.

In this work we study QS distributions for processes with an absorbing state, but without spatial structure. We find that the Malthus-Verhulst process and the contact process on a complete graph have the same scaling properties near their respective critical points. A study of Schlögl's second model illustruates how a discontinuous phase transition emerges in the infinite-size limit, associated with a rapid change in the QS distribution, which is bimodal in the vicinity of the transition. The voter model on a complete graph serves as a negative example: it has no active stationary state, and the QS distribution, which is uniform on the set of allowed density values, is very different from the true long-time distribution, even in the infinite-size limit. Our two final examples are bivariate processes. The pair approximation to the contact process shows scaling properties that are very similar to those of the complete-graph version. A study of a pair of competing Malthus-Verhulst processes reveals that mutation causes a radical change in the QS distribution.

Several directions for future work on quasi-stationary distributions can be mentioned. First, it should be possible to derive continuum equations, analogous to the Fokker-Planck equation, to describe the QS distribution in the limit of large system size. Second, analysis of QS properties for a series of system sizes promises to be a useful method for studying lattice models possessing an absorbing state. Through finite-size scaling analyses and extrapolation procedures, it should be possible to extract useful estimates of critical properties for such models. Finally, numerical study of more elaborate models used in epidemiology and population dynamics may yield a better understanding of such processes.

Acknowledgment

We are grateful to Miguel Angel Muñoz for helpful discussions. This work is supported by CNPq, Brazil.

REFERENCES

[1] van Kampen N G 1992 *Stochastic Processes in Physics and Chemistry* (Amsterdam: North-Holland)

[2] Gardiner C W 1990 *Handbook of Stochastic Methods* (Berlin: Springer-Verlag)

[3] Bartlett M S 1960 *Stochastic Population Models in Ecology and Epidemiology* (London: Methuen)

[4] Harris T E 1974 *Ann. Prob.* **2** 969

[5] Dickman R, Muñoz M A, Vespignani A and Zapperi S 2000 *Braz. J. Phys.* **30** 27

[6] Bohr T, van Hecke M, Mikkelsen R and Ipsen M 2001 *Phys. Rev. Lett.* **86** 5482, and references therein.

[7] Marro J and Dickman R 1999 *Nonequilibrium Phase Transitions in Lattice Models* (Cambridge: Cambridge University Press)

[8] Hinrichsen H 2000 *Adv. Phys.* **49** 815

[9] Schulman L S and Seiden P E 1986 *Science* **233** 425

[10] Press W H, Flannery B P, Teukolsky S A and Vetterling W T 1996 *Numerical Recipes* (Cambridge: Cambridge University Press)

[11] Binder K 1981 *Phys. Rev. Lett.* **47** 693

[12] Dickman R and Kamphorst Leal da Silva J (1998) *Phys. Rev.* E**58** 4266

[13] Muñoz M A 1998 *Phys. Rev.* E**57** 1377

[14] Schlögl F 1972 *Z. Phys.* **253** 147

[15] Brachet M E and Tirapegui E 1981 *Phys. Lett.* A**81** 211

[16] Grassberger P 1982 *Z. Phys.* B**47** 465

[17] Liggett T 1985 *Interacting Particle Systems* (Berlin: Springer-Verlag)

[18] Dornic I, Chaté H, Chave J and Hinrichsen H 2001 *Phys. Rev. Lett.* **87** 045701

[19] Dickman R 2001 *Preprint* cond-mat/0110xxxx.

FIGURE CAPTIONS

Figure 1. Probability distributions for the contact process on a complete graph, $L = 100$ sites. The curves (connecting values at integer points) represent the long-time limit of the master equation, normalized to the survival probability $P(t)$. Points represent the quasi-stationary distribution determined by the recurrence relations. Left curve: $\lambda = 1.2$; right: $\lambda = 2$.

Figure 2. Quasi-stationary population density versus λ for the contact process on a complete graph. System sizes 100, 200, 500, 1000, and 2000, top to bottom on the left-hand side. The inset is a detail of the critical region, including the curve for the infinite-size limit, $\rho - 1 - \lambda^{-1}$.

Figure 3. Quasi-stationary moment ratio m versus λ for the contact process on a complete graph. System sizes 20, 50, 100, 200, 500, and 1000, in order of increasing steepness.

Figure 4. Quasi-stationary lifetime τ versus λ for the contact process on a complete graph. System sizes 100, 500, 1000, and 5000, upper to lower on left-hand side.

Figure 5. Quasi-stationary distribution (solid line) and pseudo-stationary distribution (points) for the contact process on a complete graph, $L = 100$ sites for $\lambda = 2$ (upper), 1.5 (middle), and 1.2 (lower). The inset in the middle panel is a detail of the region near $n = 0$.

Figure 6. Quasi-stationary density versus λ for the Malthus-Verhulst process. System sizes 100, 10^3, and 10^4, upper to lower on the left-hand side. The inset shows moment ratio m versus λ for the same system sizes.

Figure 7. Scaling plot of the quasi-stationary distribution, $f = \Omega^{1/2}\overline{p}_n$ versus $y = n/\Omega^{1/2}$, at the critical point: $+$: MVP, $\Omega = 10^4$; $\circ$: contact process on complete graph, $\Omega = 10^3$; solid curve: asymptotic scaling function $f(y)$ obtained via numerical integration.

Figure 8. Quasi-stationary density versus λ for the second Schlögl process with $\mu = \nu = 1$. System sizes 100, 500, 1000, and 5000, (in order of increasing steepness). The dashed curve is the mean-field solution, which is discontinuous at $\lambda = 2$.

Figure 9. Quasi-stationary distribution for the second Schlögl process with $\mu = \nu = 1$, system size $\Omega = 1000$. $\lambda = 1.98$, 2, and 2.02 (upper to lower on left-hand

side).

Figure 10. Quasi-stationary density versus λ for the contact process in the pair approximation. System sizes 20, 40, 80, 160, 320, and 640. The inset shows moment ratio m versus λ for the same system sizes.

Figure 11. Scaling plot of the quasi-stationary distribution: $P^* = \Omega^{1/2}\overline{p}_n$ versus $n^* = n/\Omega^{1/2}$, at the critical point of the contact process. Open circles: pair approximation, $\Omega = 640$; solid line: pair approximation, $\Omega = 2560$; filled circles: contact process on complete graph, $\Omega = 1000$.

Figure 12. Quasi-stationary probability distribution for the critical contact process in the pair approximation, system size $\Omega = 40$.

Figure 13. Quasi-stationary order parameter Δ versus mutation rate q for a pair of competing MVPs at the critical point. System sizes $\Omega = 20$, 50, 100, 200, 500, 1000 (upper to lower). The inset shows $\ln \Delta$ versus $\Omega^{0.2}$ for (upper to lower) $q = 0.02$, 0.05, and 0.1.

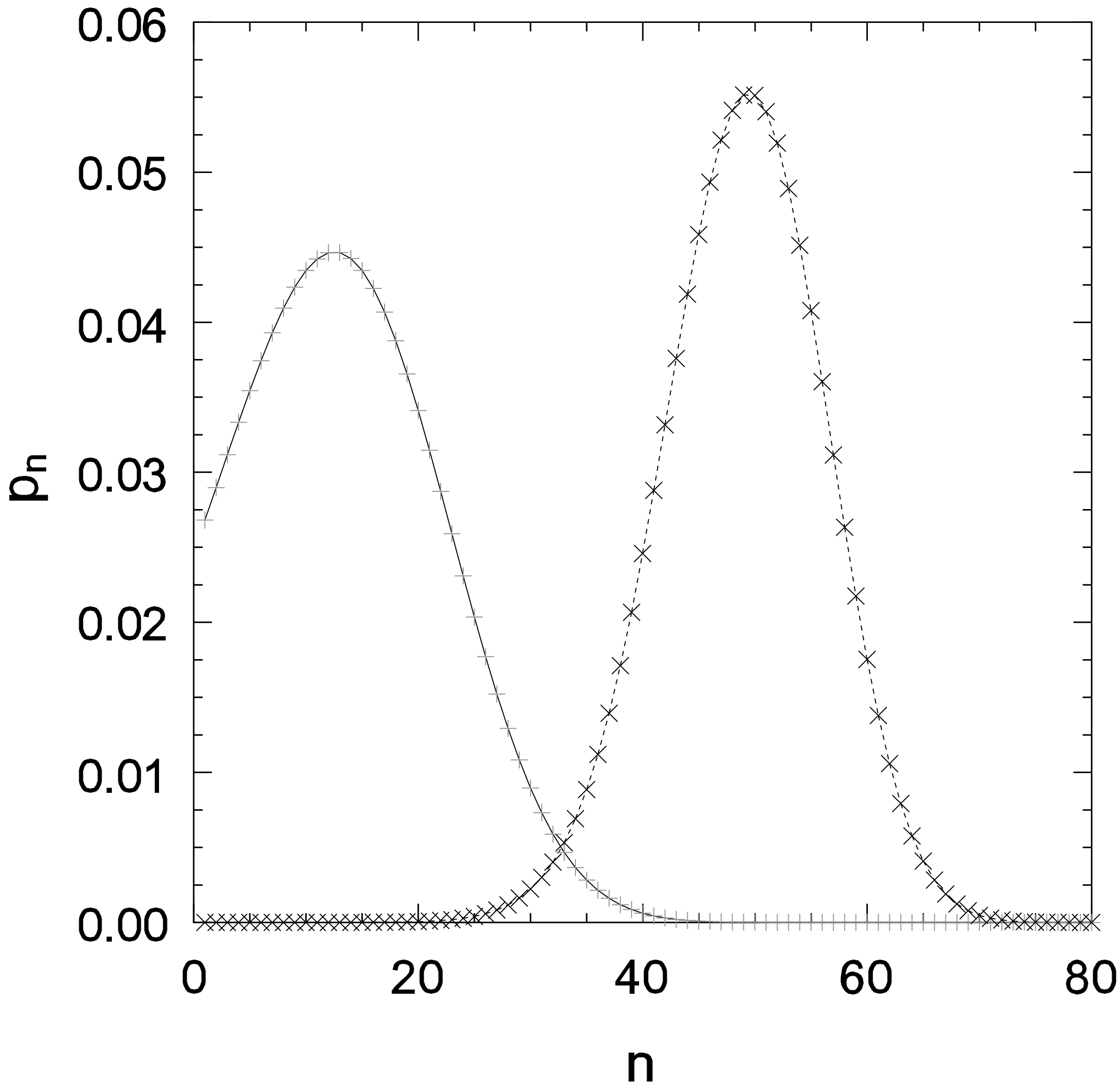
0.06
0.05
0.04
0.03
0.02
0.01
0.00
p_n
0
20
40
60
80
n

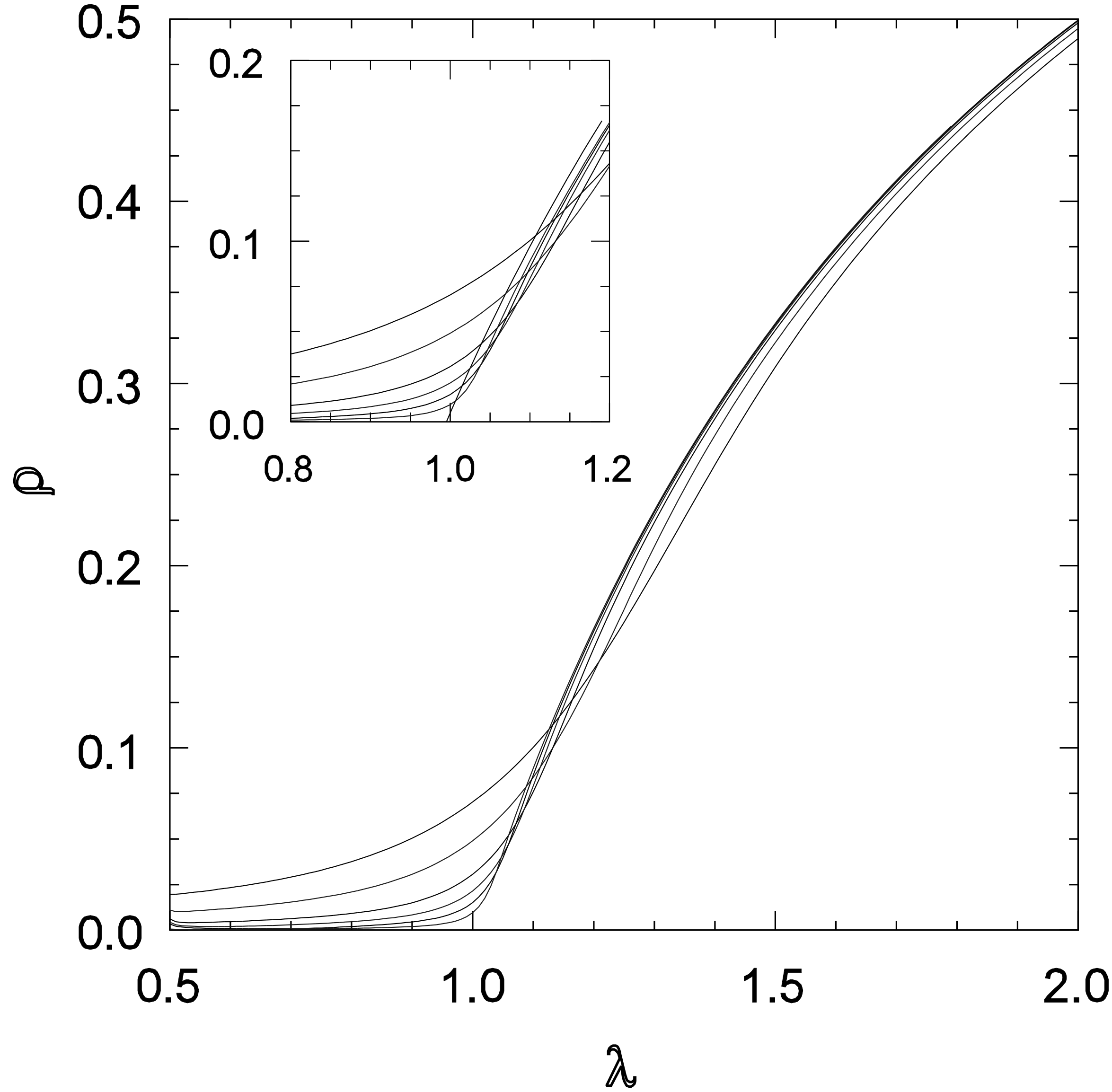

0.5
0.4
0.3
0.2
0.1
0.0
ρ
0.5
1.0
1.5
2.0
λ
0.2
0.1
0.0
0.8
1.0
1.2

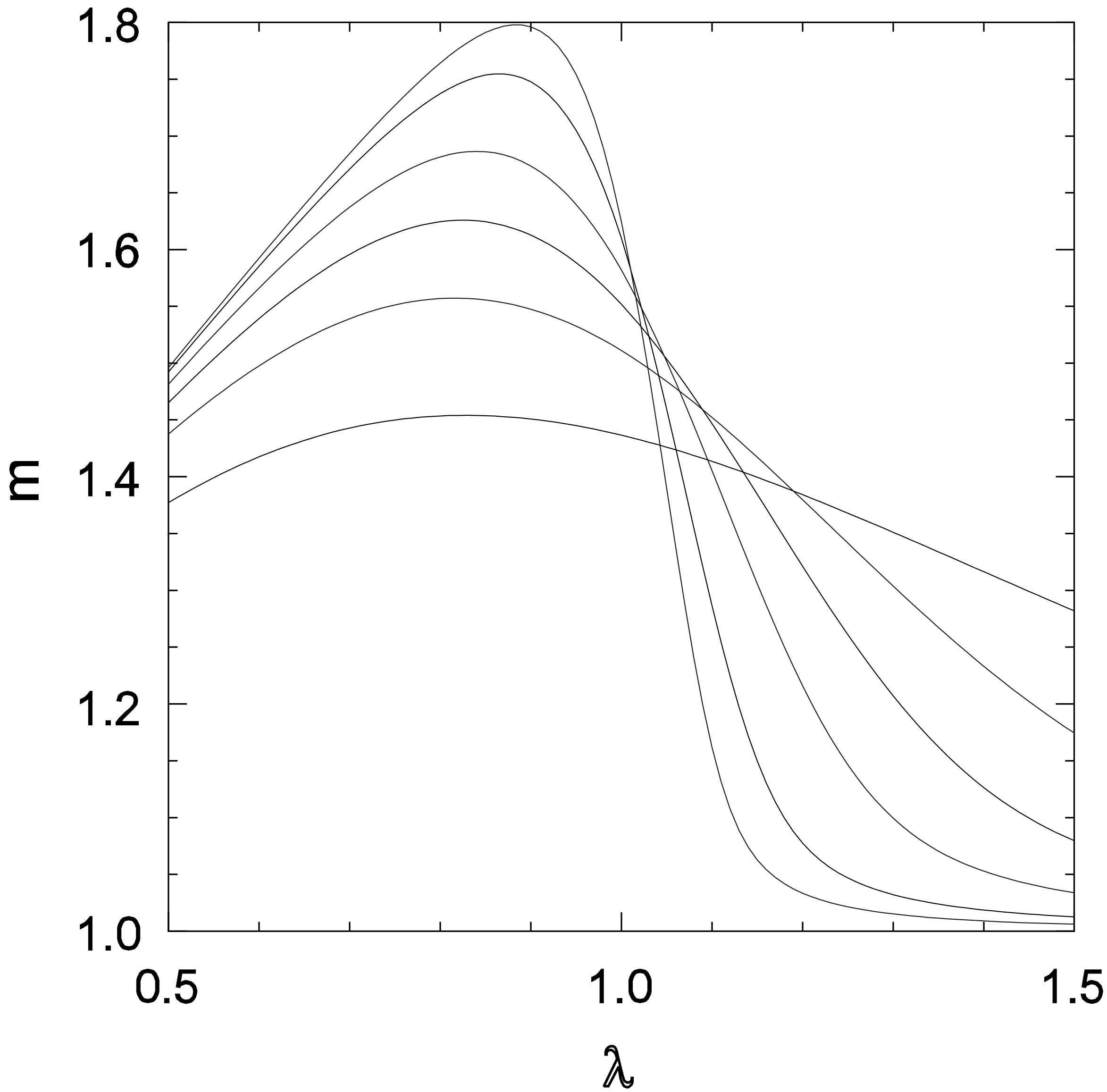
1.8
1.6
1.4
1.2
1.0
m
0.5
1.0
1.5
λ

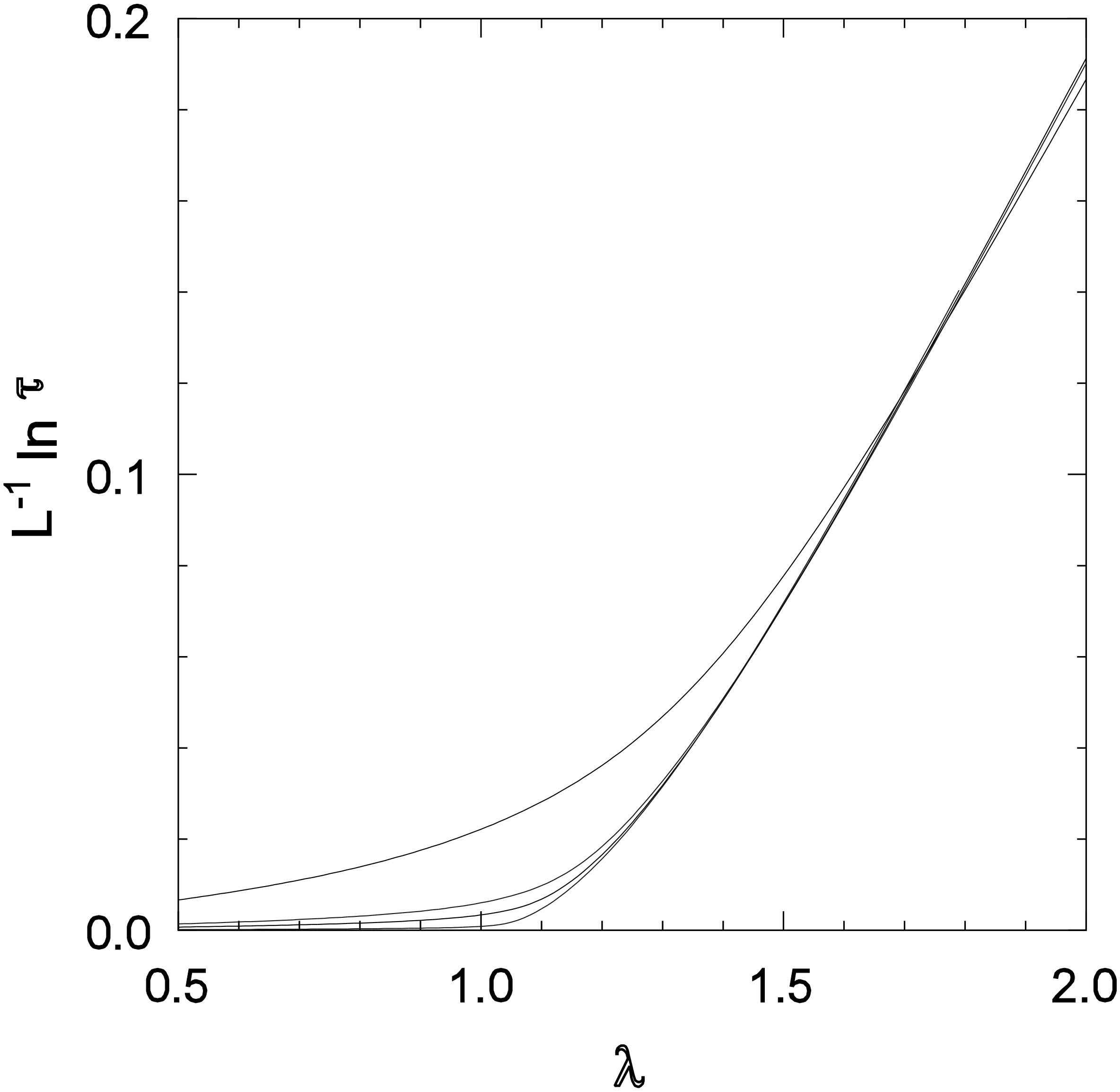

0.2
0.1
0.0
$L^{-1} \ln \tau$
0.5
1.0
1.5
2.0
λ

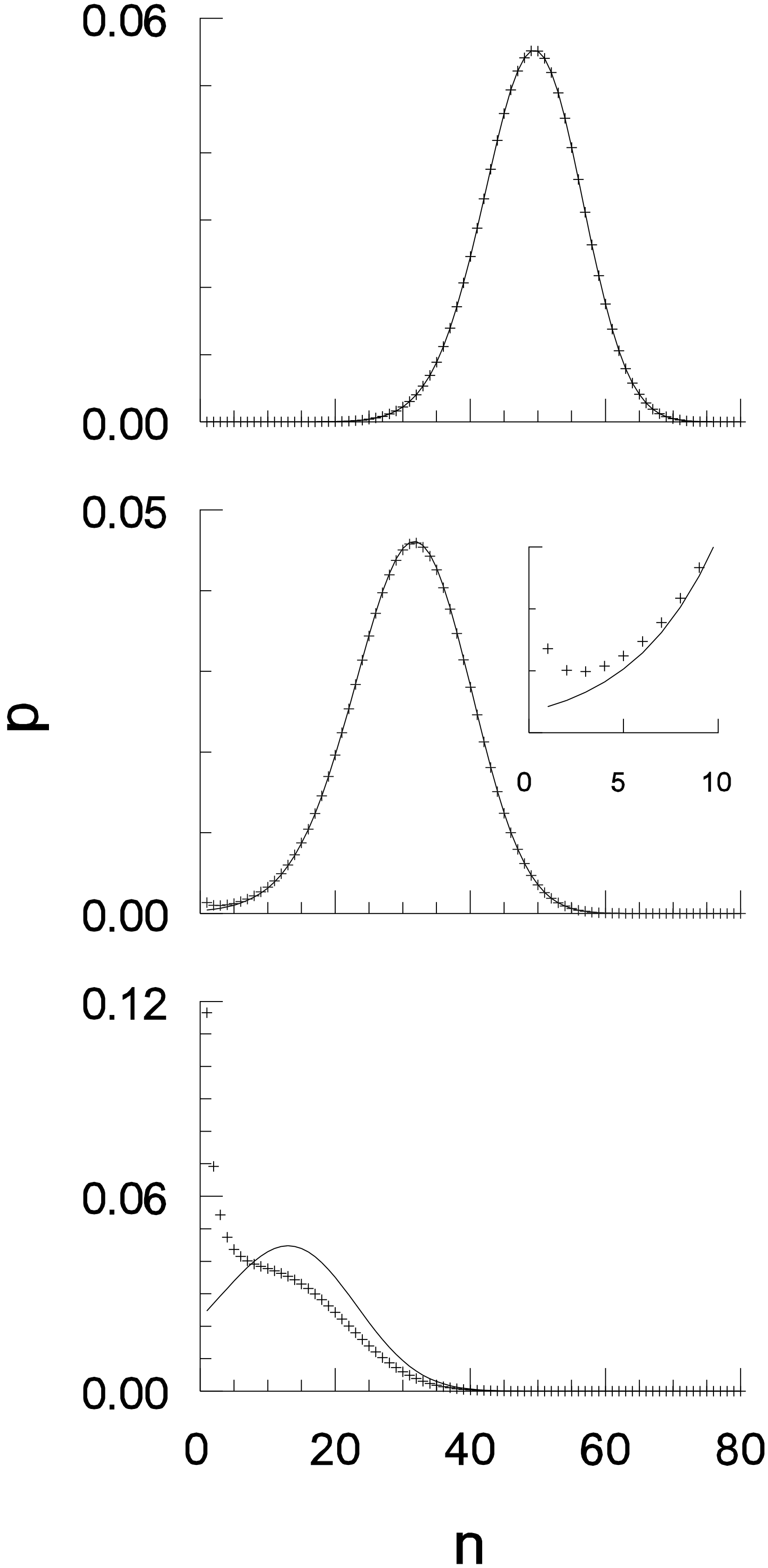
0.06
0.00
0.05
0.00
0.12
0.06
0.00
p
0
5
10
0
20
40
60
80
n

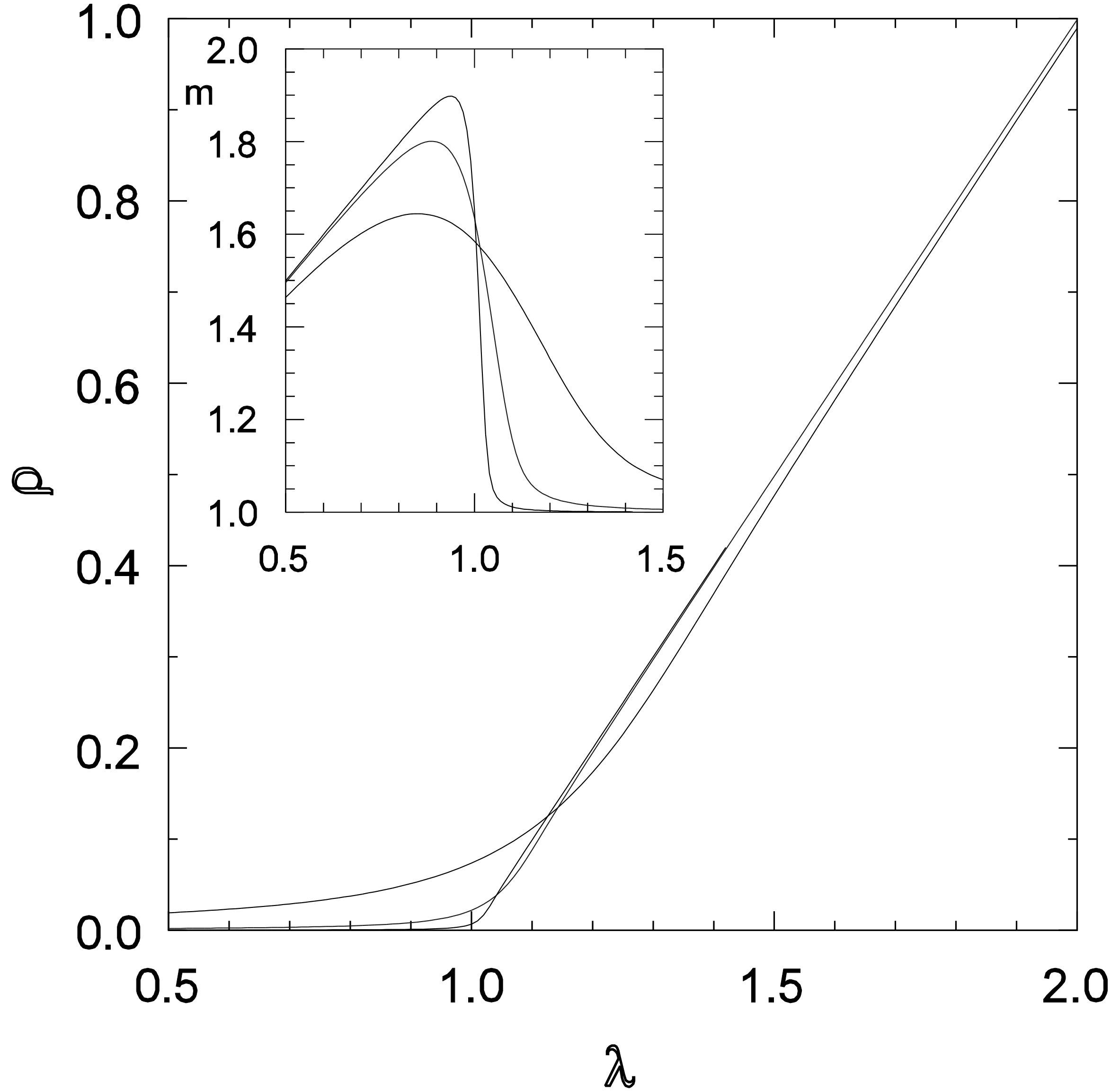

1.0
0.8
0.6
0.4
0.2
0.0
ρ
0.5
1.0
1.5
2.0
λ
2.0
m
1.8
1.6
1.4
1.2
1.0
0.5
1.0
1.5

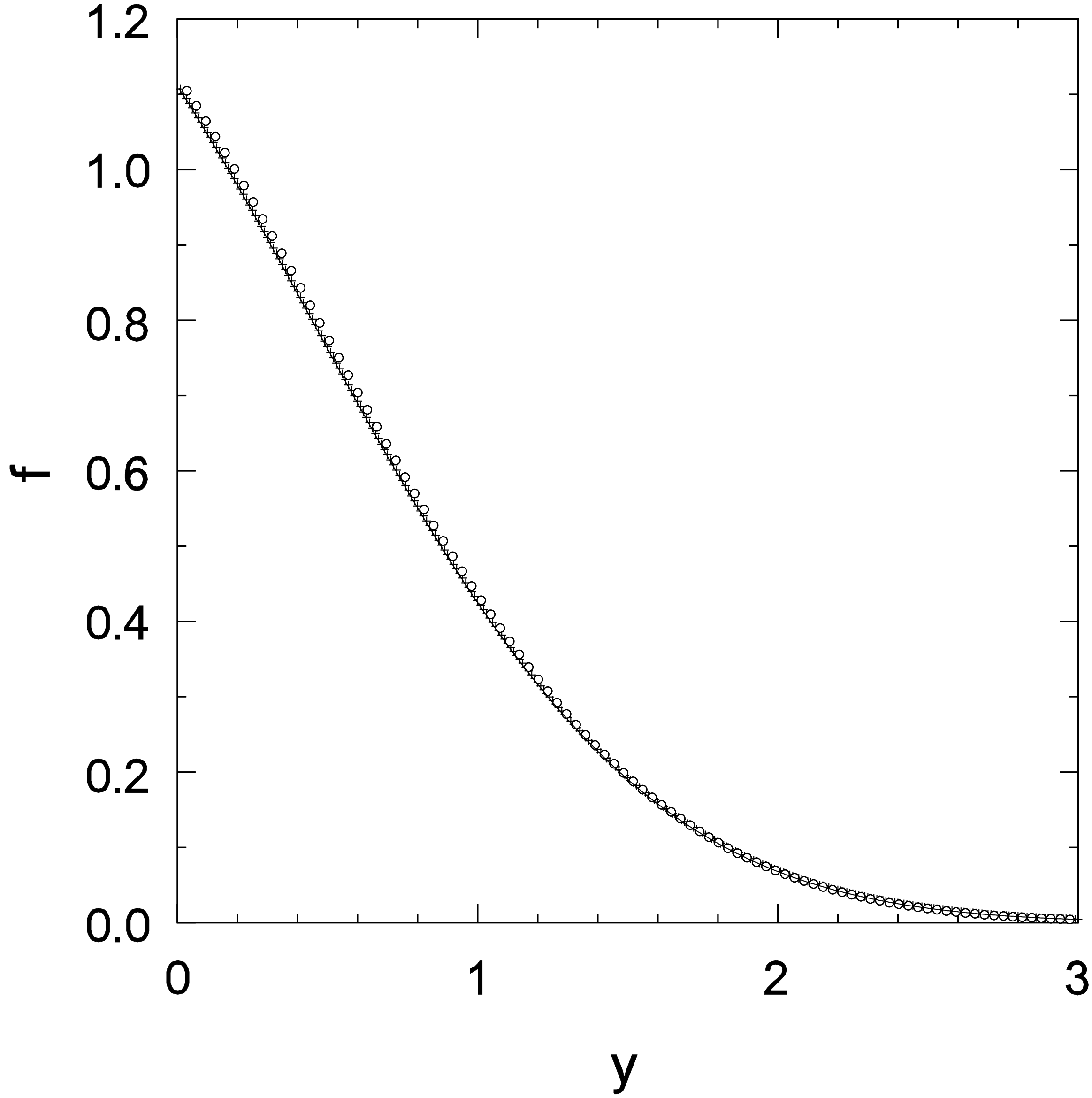

1.2
1.0
0.8
0.6
0.4
0.2
0.0
f
0
1
2
3
y

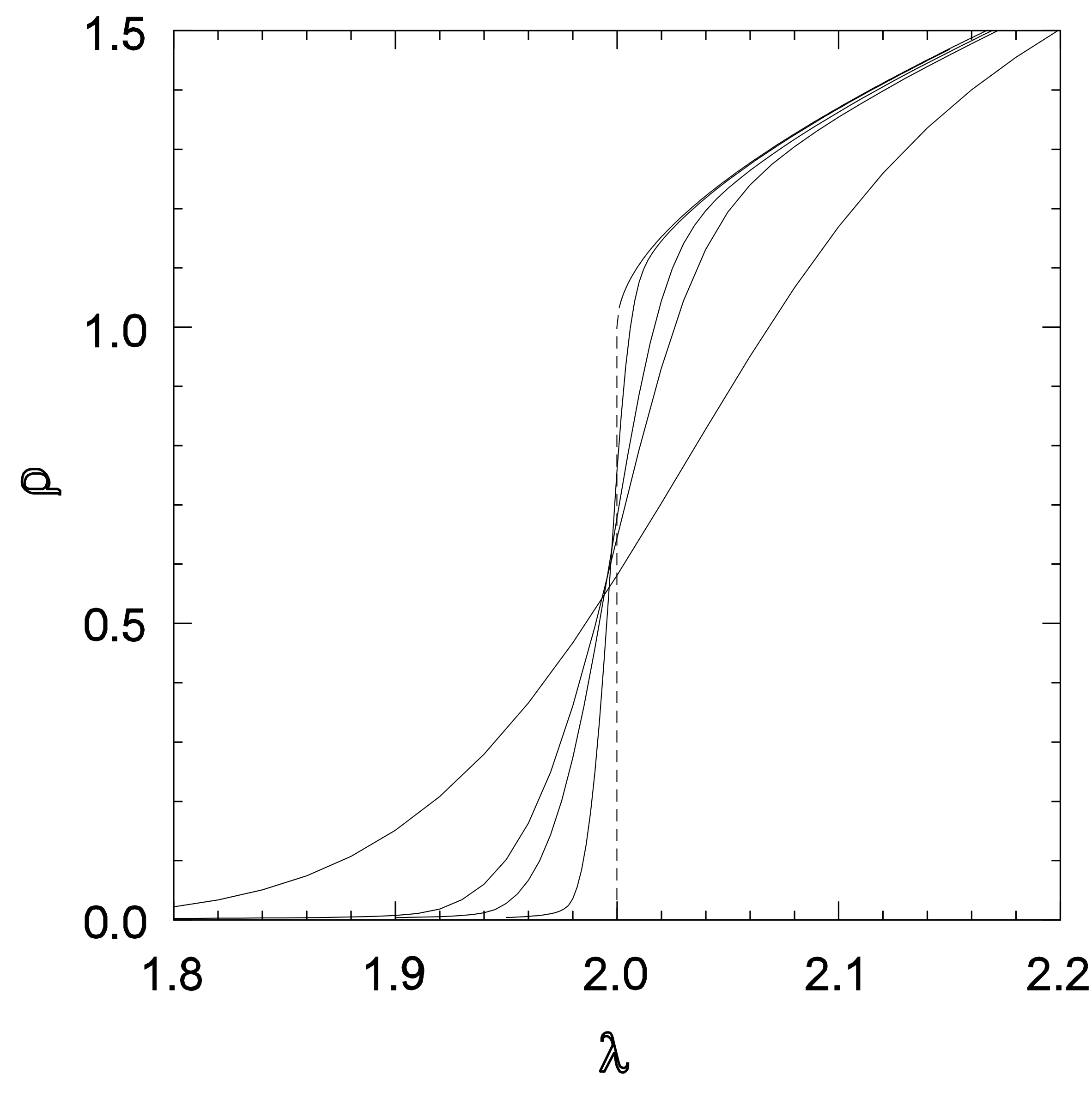

1.5
1.0
0.5
0.0
ρ
1.8
1.9
2.0
2.1
2.2
λ

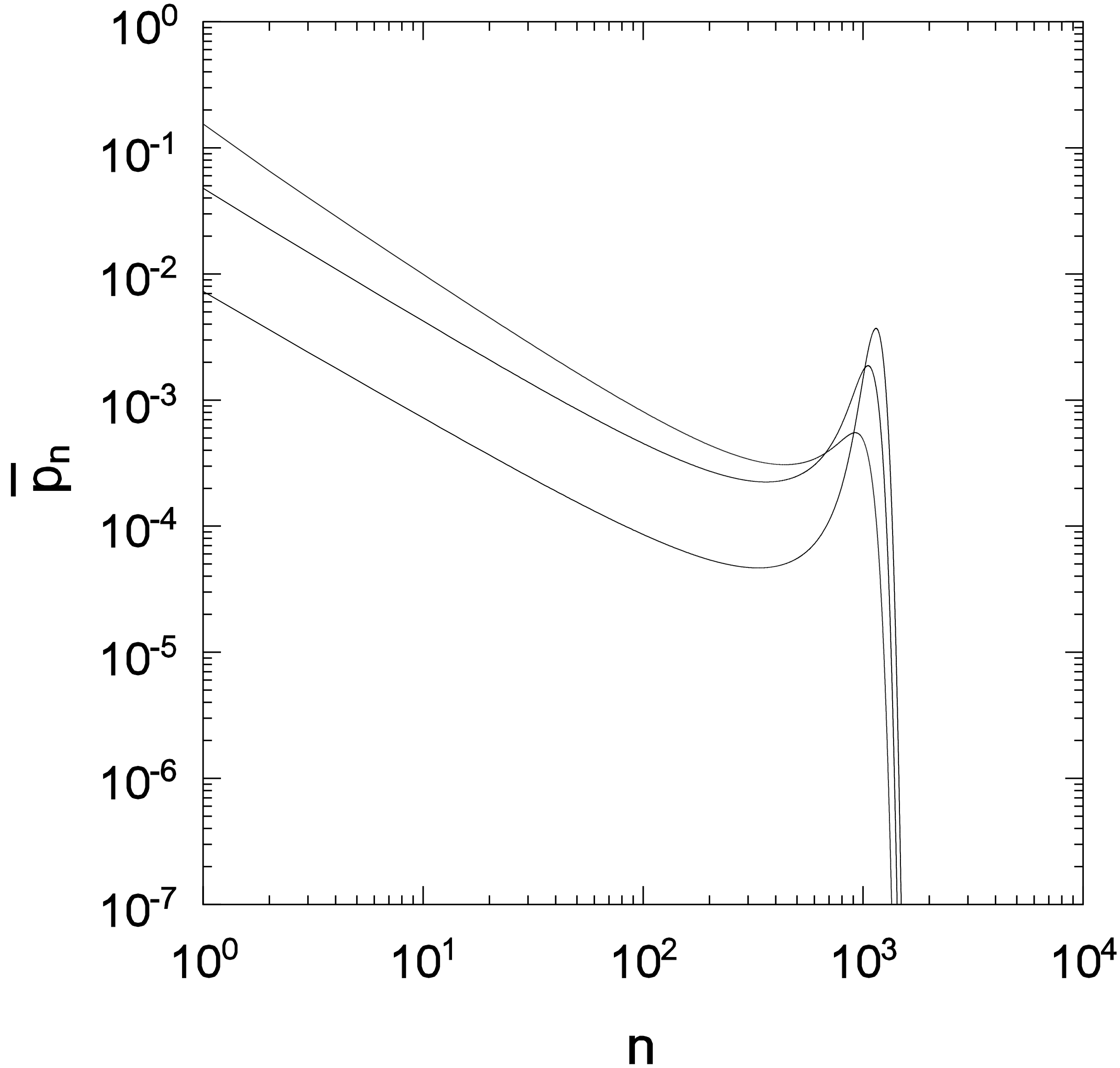

10^0
10^{-1}
10^{-2}
10^{-3}
10^{-4}
10^{-5}
10^{-6}
10^{-7}
$\bar{p}_n$
10^0
10^1
10^2
10^3
10^4
n

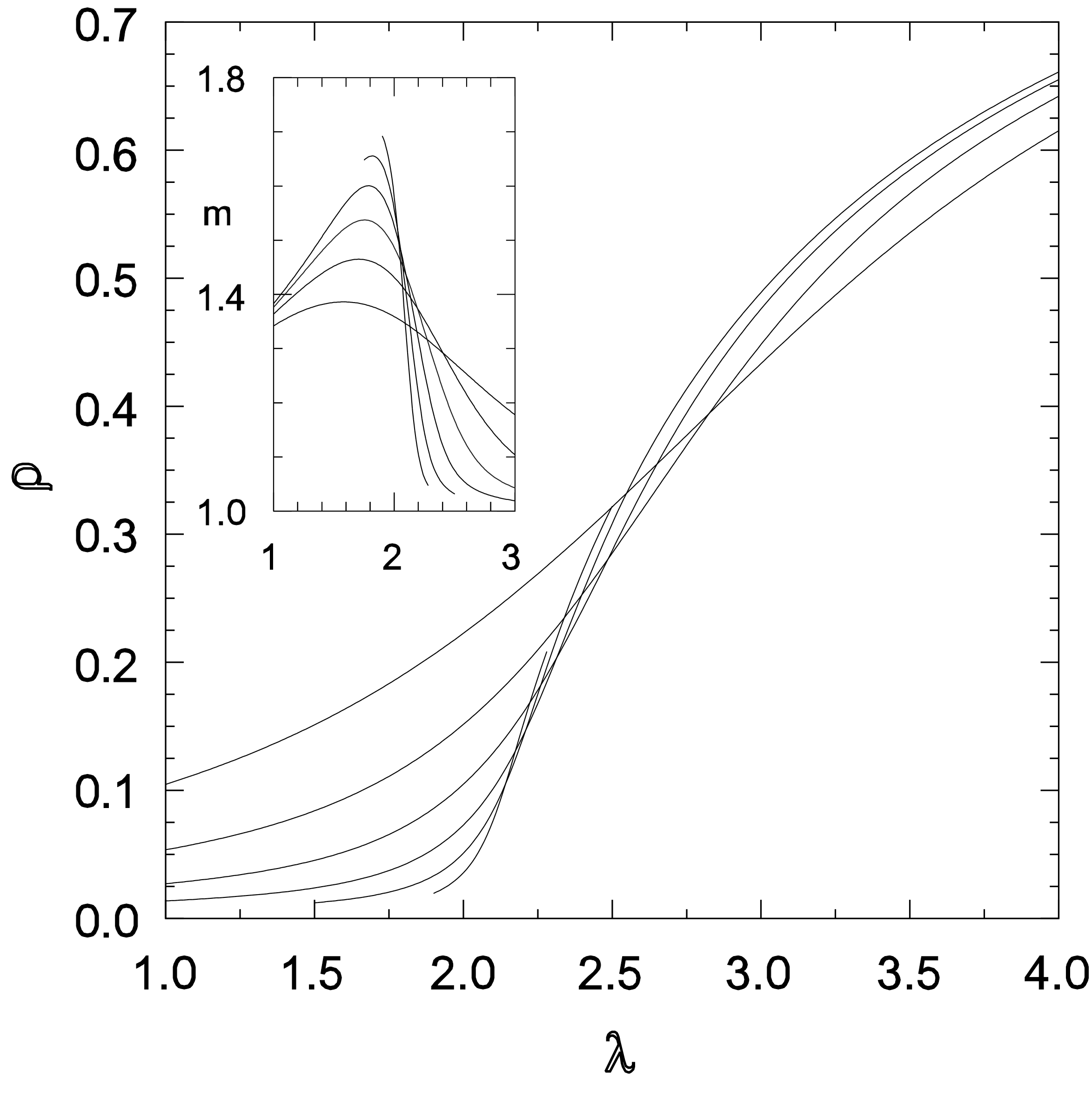

0.7
0.6
0.5
0.4
0.3
0.2
0.1
0.0
ρ
1.0
1.5
2.0
2.5
3.0
3.5
4.0
λ
1.8
m
1.4
1.0
1
2
3

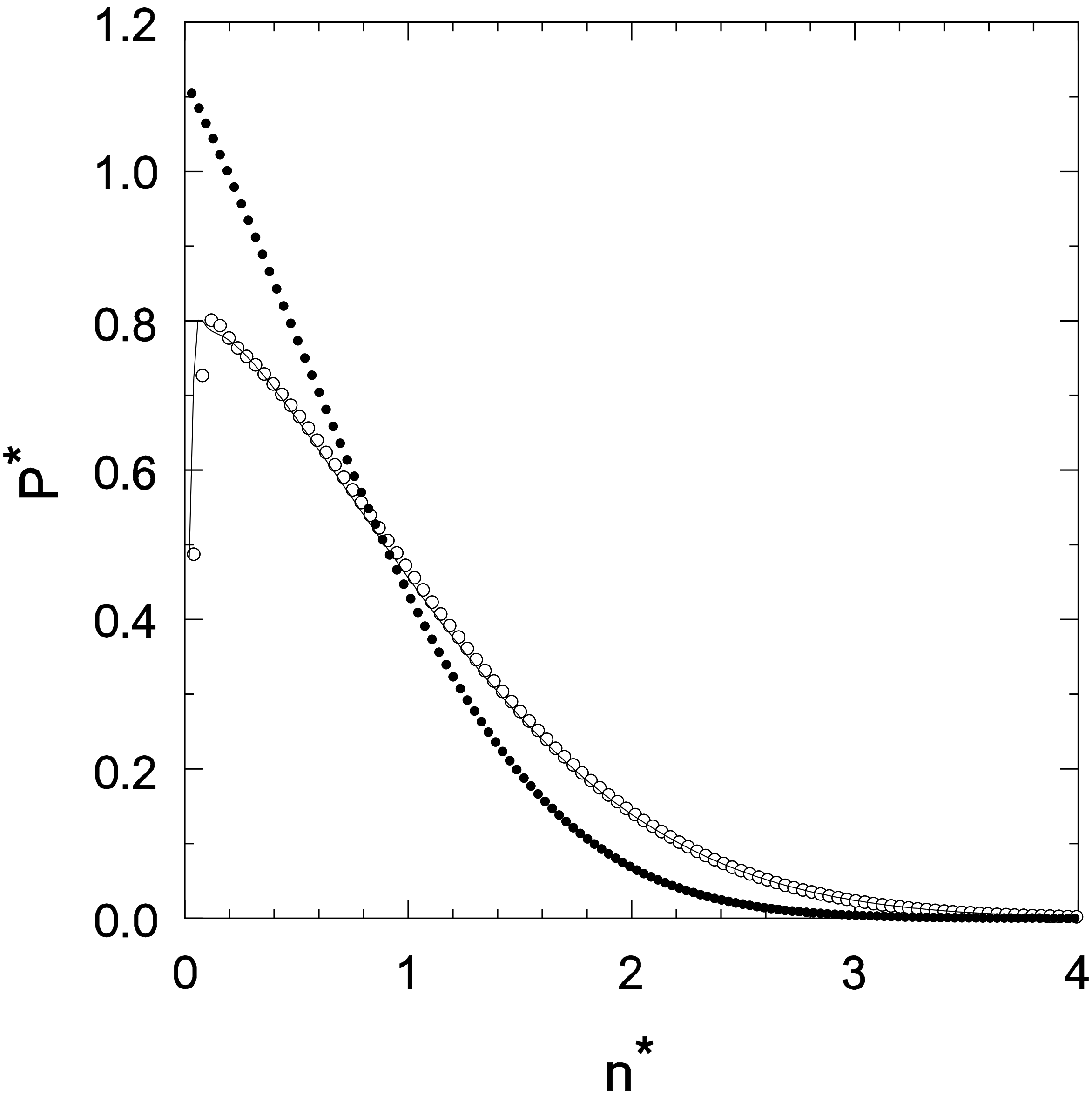

1.2
1.0
0.8
0.6
0.4
0.2
0.0
P*
0
1
2
3
4
n*

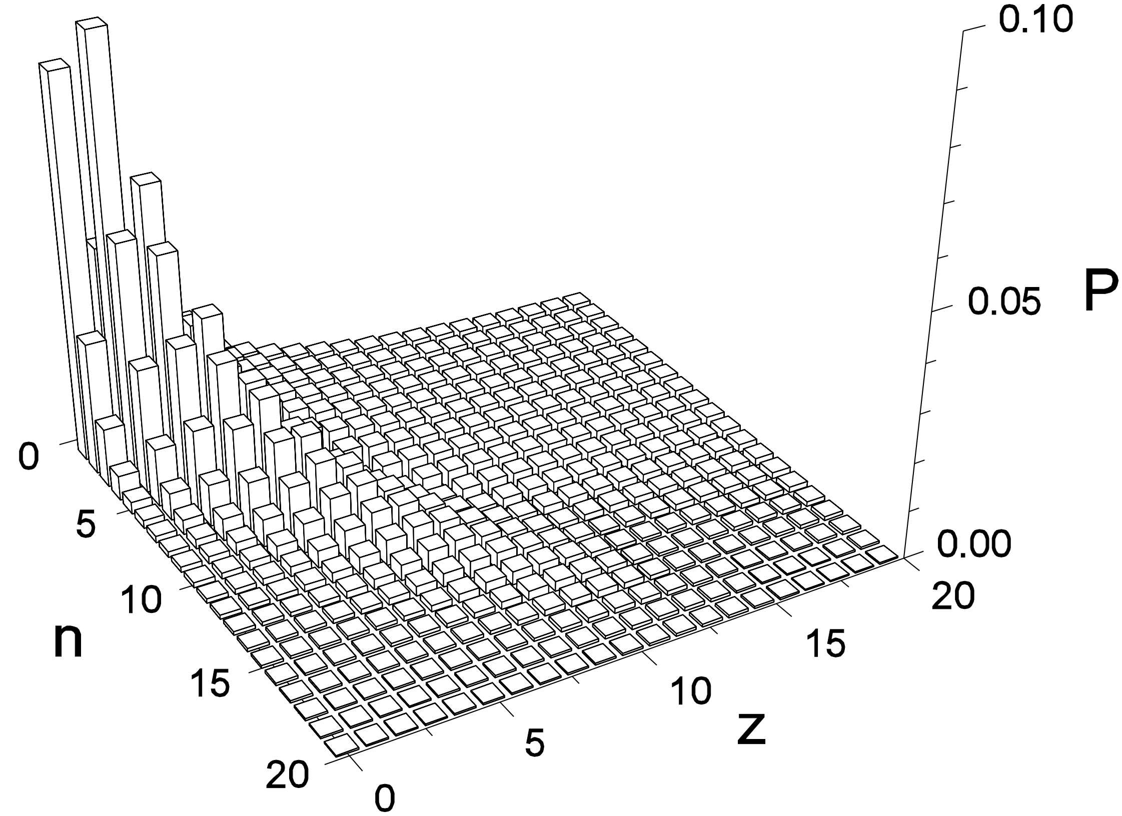
0.10
0.05
P
0.00
0
5
10
n
15
20
0
5
10
z
15
20

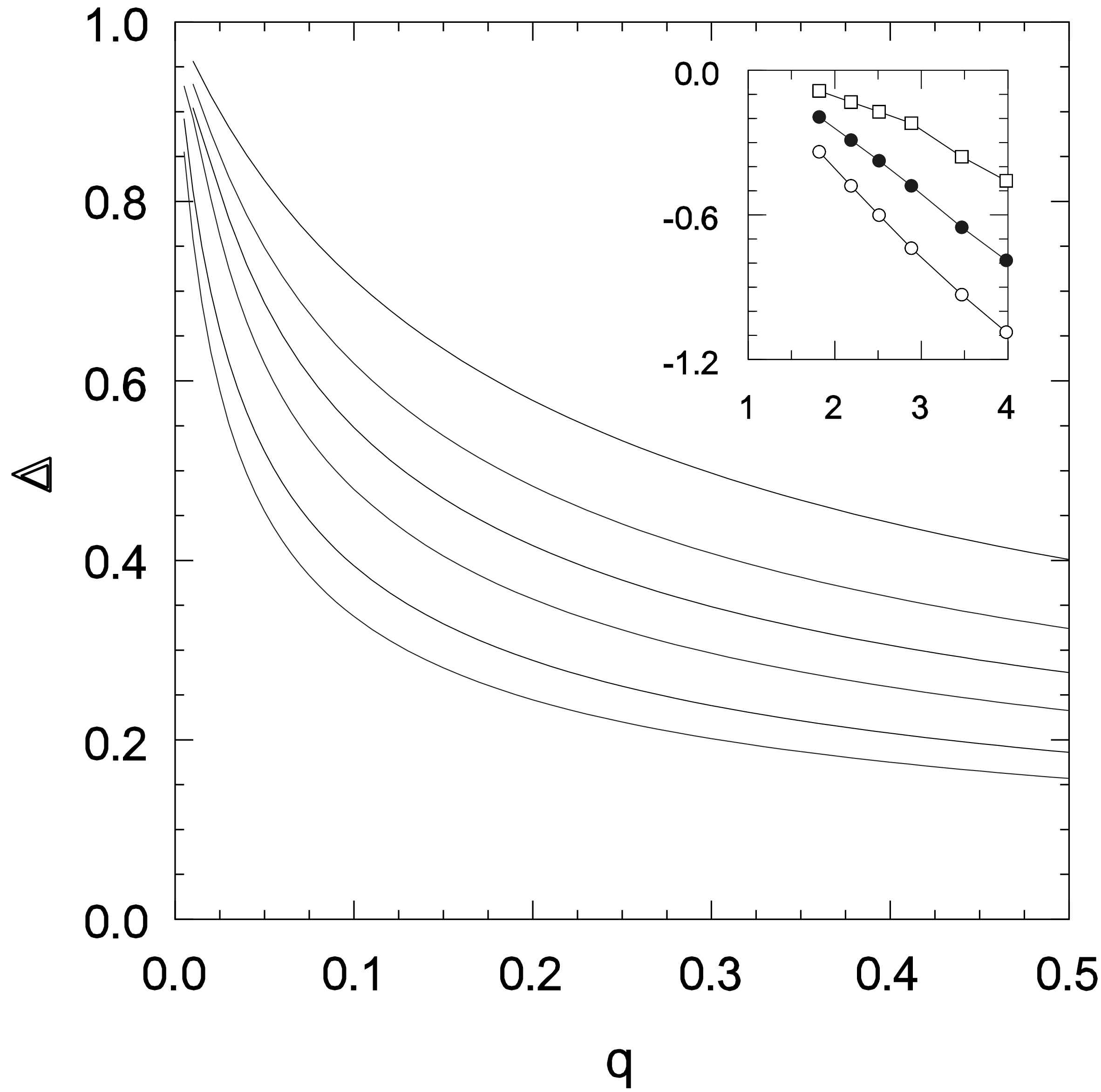

1.0
0.8
0.6
0.4
0.2
0.0
Δ
0.0
0.1
0.2
0.3
0.4
0.5
q
0.0
-0.6
-1.2
1
2
3
4